Heliyon 9 (2023) e22185

Contents lists available at ScienceDirect

Heliyon

journal homepage: www.cell.com/heliyon

Synthesis and characterization of new biocatalyst based on LDH functionalized with L-asparagine amino acid for the synthesis of *tri*-substituted derivatives of 2, 4, 5-(H1)-imidazoles

Shahram Moradi, Hadi Hassani Ardeshiri, Alireza Gholami, Hossein Ghafuri *

Catalysts and Organic Synthesis Research Laboratory, Department of Chemistry, Iran University of Science and Technology, Tehran, 16846-13114, Iran

ARTICLE INFO

Keywords:
Layered double hydroxide
Biocatalyst
Imidazole
Asparagine
Multi-component assembly

ABSTRACT

In this study, a new and recyclable biocatalyst (MgAl CO_3-LDH@Asn) was synthesized by immobilizing L-asparagine amino acid (Asn) on the surface of 3-(chloropropyl)-trimethoxysilane modified MgAl CO_3-layered double hydroxide (LDH). The physicochemical properties of the samples were identified by Fourier transform infrared (FT-IR), X-ray diffraction (XRD), scanning electron microscopy (SEM), energy dispersive X-ray (EDX), and thermogravimetric analysis (TGA) techniques. The MgAl CO_3-LDH@Asn was employed in the multi-component assembly process for the synthesis of *tri*-substituted derivatives of 2,4,5-(H1)-imidazoles from benzyl, various benzaldehyde derivatives, and ammonium acetate. For optimizing the reaction, the main factors, including the amount of MgAl CO_3-LDH@Asn, type of solvent, reaction time, and temperature were evaluated. The optimum conditions of the model reaction were achieved using 20 mg of MgAl CO_3-LDH@Asn biocatalyst in ethanol solvent after 20 min at reflux temperature. According to the findings above, the results indicated that high-yield products are achieved within a short time frame. Moreover, the high catalytic activity of the MgAl CO_3-LDH@Asn was maintained for four cycles without significantly diminishing its performance.

1. Introduction

Nowadays, layered double hydroxides (LDHs) have attracted considerable attention as solid catalysts, and have applications in various organic processes [1–5]. LDHs are host–guest materials composed of generic layer sequence $[M^{II}_{1-x}\ M^{III}_{x}(OH)_2]^{x+}\ [A_{x/n}]^{n-}.\ mH_2O$, in which A^{n-} are non-framework inorganic or organic anions, M^{II} and M^{III} are the divalent and trivalent metal ions, respectively, m is the number of interlayer water, and $x = M^{3+}/(M^{2+}+M^{3+})$ is molar ratio that typically ranges from 0.2 to 0.3 [6,7]. There are other types of LDH based on tetravalent cations. Although not as common as trivalent cations, some tetravalent cations, such as Zr^{4+} and Sn^{4+}, have been introduced into brucite-type layers to replace some trivalent cations in LDH compounds [8]. A significant characteristic of LDH is the absence of cross-linking between cations layers, which allows them to host a broad range of intercalary anions [9]. The partial substitution of trivalent by divalent cations leads to a positive sheet charge, compensated by anions located in the interlayer galleries [10,11]. From a thermodynamic perspective, the exchange of anions in LDHs depends on the electrostatic interplay among the exchangeable anions and the positive charge of the cations [12]. LDHs, due to their interesting properties in anion

* Corresponding author.
E-mail address: Ghafuri@iust.ac.ir (H. Ghafuri).

https://doi.org/10.1016/j.heliyon.2023.e22185
Received 23 June 2023; Received in revised form 5 November 2023; Accepted 6 November 2023
Available online 11 November 2023
2405-8440/© 2023 Published by Elsevier Ltd. This is an open access article under the CC BY-NC-ND license (http://creativecommons.org/licenses/by-nc-nd/4.0/).

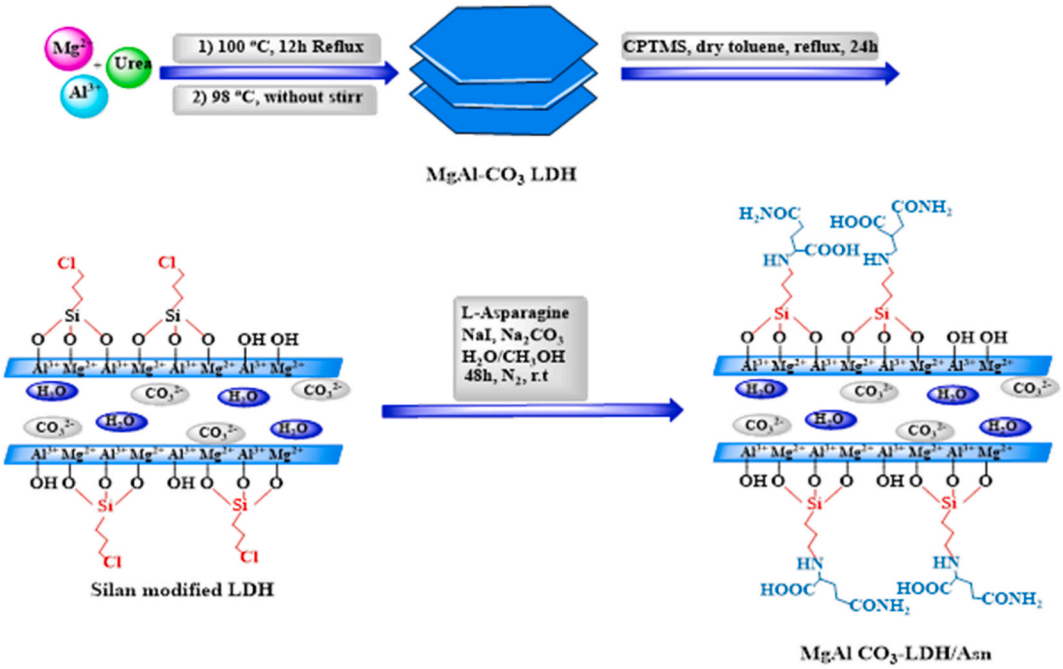

Scheme 1. Preparation process of the MgAl CO_3-LDH-CPTMS@Asn nanocomposite.

exchangeability, compositional flexibility, and biocompatibility, have attracted great attention as a catalyst support or precursor in the heterogeneous catalysis fields, such as thermo–photocatalysts [13,14], electrocatalysts [15], advanced oxidation processes (AOPs) [16], etc. Due to the lack of functional groups and structural components of pristine LDH, adsorption capability and other LDH applications are limited [17]. To solve this issue, functionalized LDH has been prepared by introducing functional groups or structural components [18]. Amino acids are suitable chelators that could be used as chelating agents with numerous functional groups in heterogeneous catalysts [19]. L-asparagine (abbreviated as Asn) is an α-amino acid used for protein bio-synthesis. It possesses an α-amino group (which is protonated as NH_3^+ under biological conditions), an α-carboxylic acid group (which is in the form of –COO– deprotonated under biological conditions), and a lateral chain carboxamide, which is classified as polar aliphatic amino acids (at physiological pH) [20,21]. LDHs are capable of electrostatic and chemical interaction with functional groups or structural constituents of L-asparagine amino acid owing to the presence of hydroxyl groups on the surface and positive octahedral charged [$Mg(OH)_6$]. Thus, L-asparagine has been intercalated in between the interlayer of LDHs, and utilized as a biocompatible and non-toxic biocatalyst for the synthesis of derivatives of 2, 4, 5-(H1)-imidazoles. Recently, various approaches have been extended for the synthesis of 2,4, 5-(H1)-imidazoles [22–25]. The best reported synthesis pathway of 2,4,5-(H1)-imidazoles is multi-component reactions (or multi-component assembly process) of benzyl, aldehyde, and ammonium acetate [26]. In continuation of our previous research on the synthesis and application of LDH-based heterogeneous catalyst [27], in this work, a new biocatalyst (MgAl CO_3-LDH@Asn) has been prepared by the immobilization of the modified MgAl CO_3-layered double hydroxide (LDH) on L-asparagine amino acid (Asn). Several analyses were carried out to evaluate its proper synthesis and immobility. We developed the synthesis of 2, 4, 5-(H1)-imidazoles *via* the three-component reaction of benzyl, various aldehyde derivatives, and ammonium acetate along with MgAl CO_3-LDH@Asn at reflux temperature. The key parameters of the model reaction, such as biocatalyst dosage, the type of solvent, the reaction temperature, and the recovery of the biocatalyst, were also investigated. The prepared biocatalyst displayed significant advantages, such as excellent efficiency, short reaction time, and catalyst recyclability.

2. Experimental section

2.1. Materials and characterizations methods

All chemical materials used in this initiative were purchased from Merck and Sigma Aldrich chemical companies without further purification, except for several aldehyde derivatives such as benzaldehyde, which were used after distillation. Chemical bonds and substance composition have been detected utilizing KBr pellets with an FT-IR spectrometer (Shimadzu 8400 s) from 400 to 4000 cm^{-1}. The X-ray diffraction (XRD) patterns of the materials were determined using Cu Ka radiation (k = 1.542A°) with the Bragg angle ranging from 5° to 80° (TW 1800). The surface topography of the samples was evaluated *via* SEM analysis (TESCAN-MIRA3). To identify the constituent elements of the biocatalyst, EDX analysis was used (Numerix DXP-X10P). Furthermore, ^{1}H NMR spectra data were compared with data obtained from the literature with a 500 MHz, Bruker DRX-500 Advance spectrometer in DMSO.

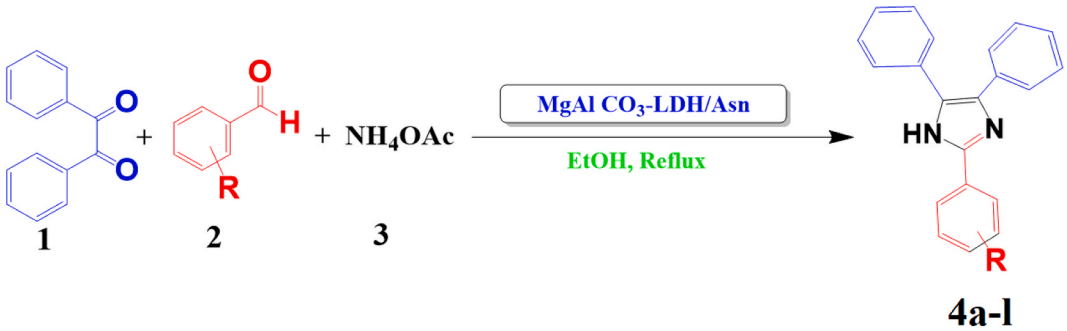

Scheme 2. Synthesis of *tri*-substituted derivatives of 2, 4, 5-(H1)-imidazoles (4a-l) catalyzed with MgAl CO_3-LDH@Asn biocatalyst through the three-component reaction between benzyl (1 mmol), benzaldehyde (1 mmol), ammonium acetate (5 mmol) in EtOH solvent at reflux temperature.

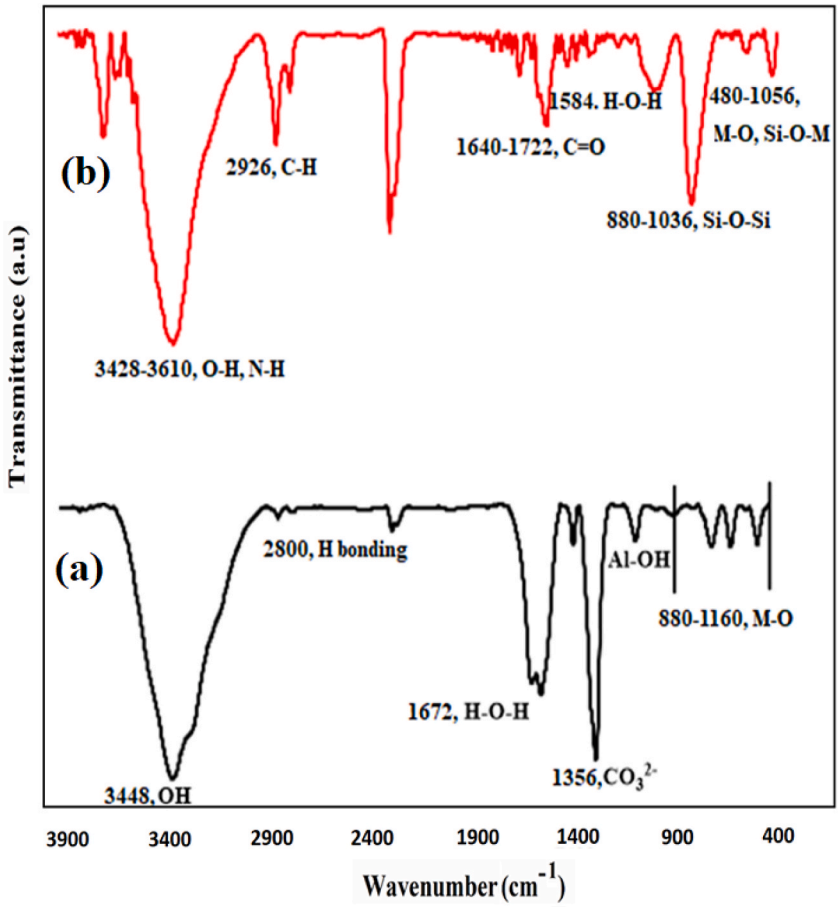

Fig. 1. FT-IR spectra of (a) MgAl CO_3-LDH and (b) MgAl CO_3-LDH@Asn biocatalyst.

2.2. Preparation of MgAl CO_3-LDH

Preparation of MgAl–CO_3-LDH with cationic metals of Mg^{2+}/Al^{3+} (molar ratio of 2:1) was carried out using a urea-assisted co-precipitation method. Initially, 5.13 g (20 mmol) of $Mg(NO_3)_2.6H_2O$ and 3.75 g (10 mmol) of $Al(NO_3)_3.9H_2O$ were dissolved in a water-based solution of urea (3 M, 100 mL). Afterward, the resulting mixture was transferred to a round-bottomed flask (200 mL) equipped containing a reflux condenser, and stirred at 100 °C for 12 h under a nitrogen atmosphere. The temperature was maintained at 94 °C for 12 h without stirring until a precipitate formed. Subsequently, the resultant suspension was centrifuged and the sediment obtained washed with methanol (MeOH) and deionized water to reach a pH = 7, then dried at 80 °C for 12 h.

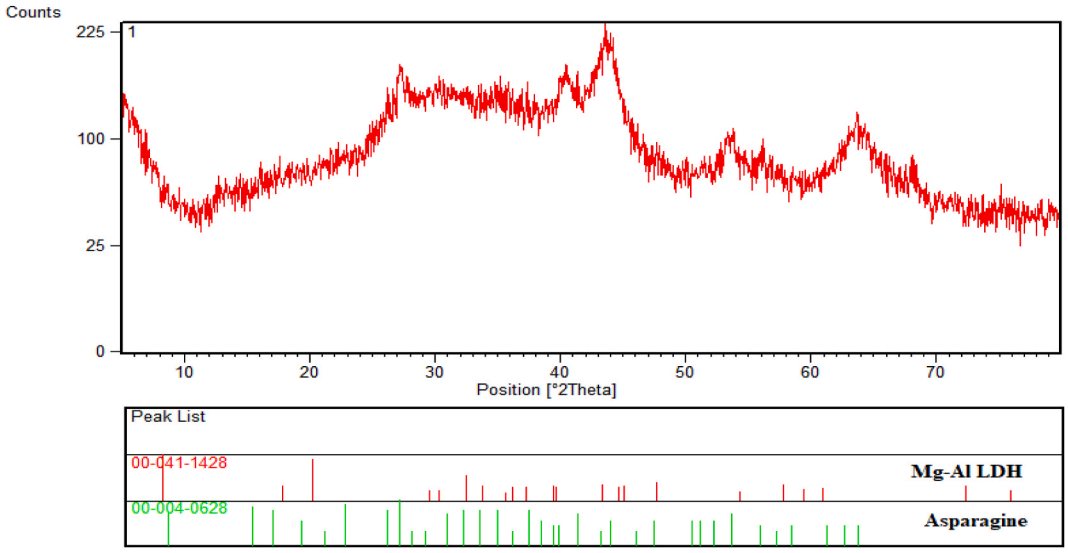

Fig. 2. XRD pattern of MgAl CO_3-LDH@Asn biocatalyst.

2.3. Preparation of MgAl CO_3-LDH-CPTMS

In a round-bottom flask, 1.00 g of MgAl–CO_3 LDH was well dispersed in an ultrasonic bath containing 50 mL of dry toluene. Thereafter, 2 mL of 3-(chloropropyl)-*tri*-methoxysilane (CPTMS) was added drop-wise to the suspension using a syringe at 90 °C under an N_2 atmosphere. Subsequently, the resulting mixture was heated at 90 °C for 24 h. Eventually, the precipitate formed was centrifugally separated and washed several times with dry toluene and dried in a vacuum oven at 60 °C.

2.4. Preparation of MgAl CO_3-LDH@Asn

To synthesis of functionalized MgAl CO_3-LDH with the L-asparagine amino acid, 1.00 g of chlorinated MgAl CO_3-LDH was thoroughly dispersed in a mixture of water and methanol (1:1) by ultrasonic. Then, L-asparagine (1 mmol), Na_2CO_3 (1 mmol), and NaI (1 mmol) were added to the reaction mixture and stirred at room temperature (r.t) under N_2 atmosphere for 48 h. Finally, the obtained solid was centrifuged and washed several times with deionized water and MeOH, and dried at room temperature (r.t) (Scheme 1).

2.5. General method for the synthesis of tri-substituted derivatives of 2,4,5-(H1)-imidazoles

In a round-bottom flask, 20 mg of MgAl CO_3-LDH@Asn biocatalyst was well dispersed in 5 mL of ethanol (EtOH). Afterward, various aldehydes (1 mmol), benzyl (1 mmol), and ammonium acetate (5 mmol) were added to the prepared nanocatalyst solution. Subsequently, the reaction vessel was agitated for 20 min in an oil bath at reflux temperature by a magnetic stirrer. The progression of the reaction was controlled by TLC chromatography with sampling and normal hexane/ethyl acetate solvents (ratio of 1:2). Once the reaction had stopped, the biocatalyst was centrifuged, washed with MeOH, and dried for further reactions. Moreover, the final products were dissolved in EtOH and re-crystallized again for further purification (Scheme 2).

3. Results and discussion

3.1. Characterization of MgAl CO_3-LDH-Asn

3.1.1. FT-IR spectra

The FT-IR spectra for (a) MgAl CO_3-LDH and (b) MgAl CO_3-LDH@Asn are represented within the wavenumber range of 400–4000 cm^{-1} (Fig. 1). In the FT-IR spectrum of MgAl CO_3-LDH (Fig. 1a), The broad absorption band is observed in the region of 3448 cm^{-1}, which is allocated to the stretching vibrations of the O–H group caused by interlayer water molecules and the hydroxyl groups in brucite-like layers [28,29]. The characteristic peak at 1672 cm^{-1} is related to the bending vibrations of the interlayer water molecule (HOH). Moreover, the characteristic peak situated at 1356 cm^{-1} is corresponded to the stretching vibrations of CO_3^{2-} and/or NO_3^- [30,31]. This peak may only be related to CO_3^{2-}, since NO_3^- anion is eliminated from the environment through urea hydrolysis and ammonia production. Furthermore, the peak appearing at 2800 cm^{-1} is assigned to the hydrogen bond between water molecules and carbonate anion [32]. The characteristic peaks at frequencies of 880–1160 cm^{-1} are linked to the vibration modes of the M − O bonds. According to Fig. 1b, the vibration frequencies at 3428-3610 cm^{-1} were allocated to the OH and NH groups. Additionally, the peaks observed at frequencies of 1470–1558 cm^{-1} are correlated with the N–H group of amino acids [33]. Absorption bands at 2926, 1640,

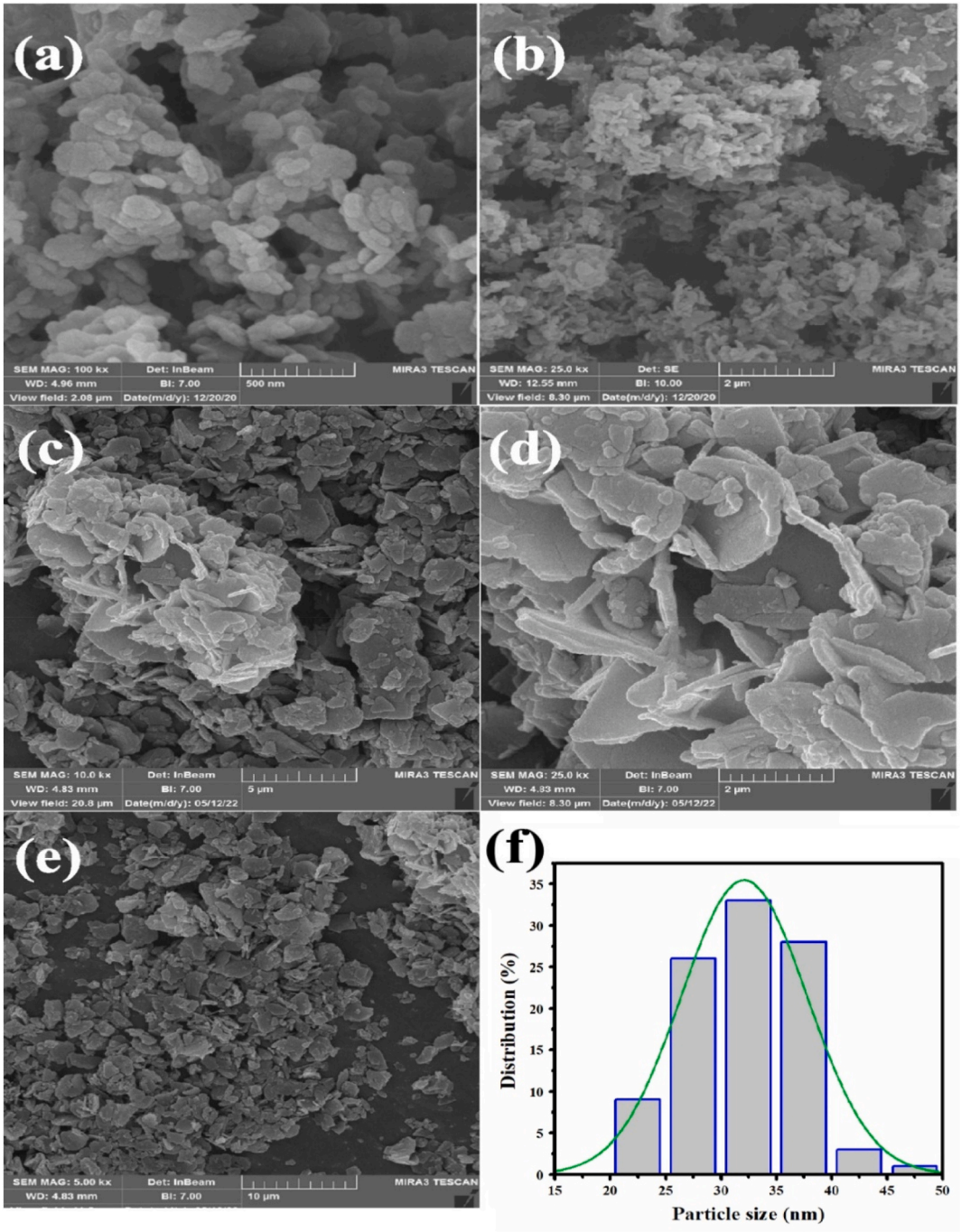

Fig. 3. SEM images of (a,b) Mg–Al LDH, (c,d,e) MgAl CO_3-LDH@Asn biocatalyst, and (f) histogram diagram of the MgAl CO_3-LDH@Asn.

and 1722 are attributed to the aliphatic C–H group (sp3), amide and acidic carbonyl (C═O) groups. Moreover, the bands located at 880-1036 cm^{-1} are attributed to the symmetric and asymmetric stretching vibrations of the Si–*O*–Si group. Furthermore, the peaks in the 480-1056 cm^{-1} area are linked and attributed to the vibrations of the M − O and Si–*O*-M bonds.

3.1.2. XRD analysis

The XRD technique was evaluated within the scanning range of $5^\circ \leq 2\theta \leq 80^\circ$ to confirm the crystalline structure of the MgAl CO_3-LDH@Asn biocatalyst (Fig. 2). The diffraction patterns at 2θ values of 11, 21, 29, 30, 38, 45, 70, and 75° were matched well with the structure of MgAl CO_3-LDH as indexed with the JCPDS card No. 00-041-1428 [34,35]. Several peaks at 2θ values of 12, 15, 25, 29, 41, 45, 54, 54, 56, and 65° are attributed to the L-asparagine amino acid (Asn) with the JCPDS card No. 00-004-0628. The crystal size of the

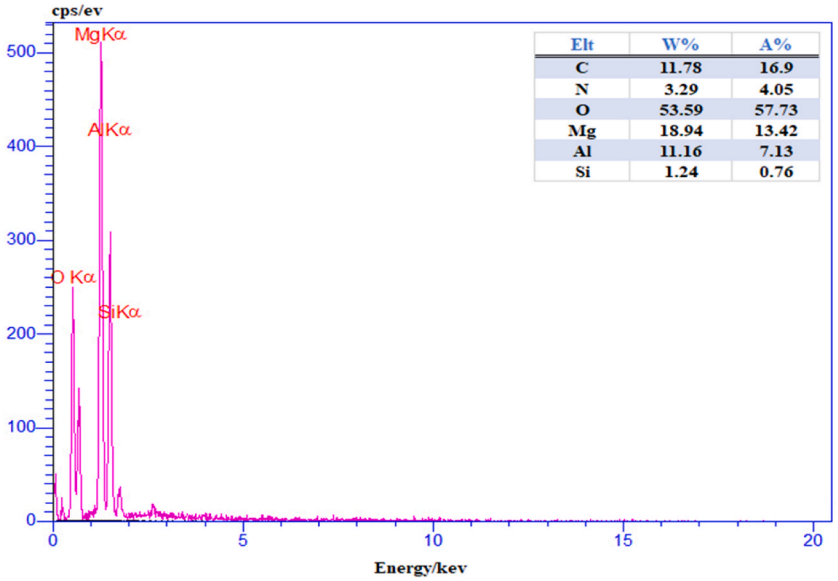

Fig. 4. EDX analysis of MgAl CO_3-LDH@Asn biocatalyst.

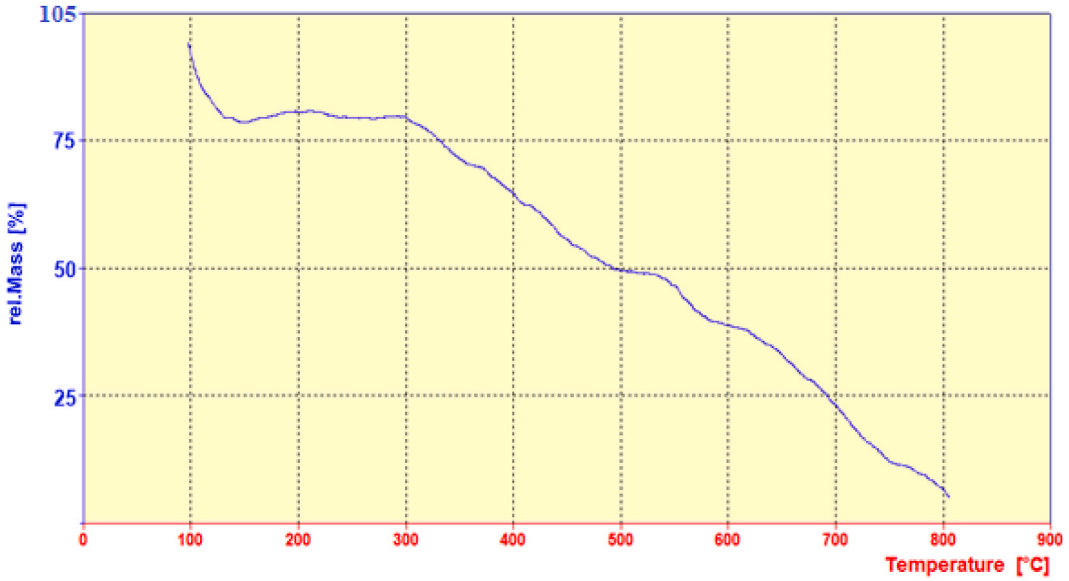

Fig. 5. TGA curve of the MgAl CO_3-LDH@Asn biocatalyst.

MgAl CO_3-LDH@Asn biocatalyst was calculated by the Scherer formula as follows:

$$D = \frac{K\lambda}{\beta \cos\theta} \quad (1)$$

Where D is the average crystallite size (nm), K is the shape factor and is equivalent to 0.89, β is full width at half the maximum intensity (FWHM) in radius, and θ is Bragg angle [36–38]. Using this formula, the crystallite size value of the MgAl CO_3-LDH@Asn particles has been calculated approximately 33 nm.

3.1.3. Morphological observations

The morphology, shape, and particle size of the MgAl CO_3-LDH@Asn biocatalyst were studied using the SEM analysis, which is illustrated in Fig. 3. The MgAl CO_3-LDH images (Fig. 3a and b) provide evidence that the MgAl CO_3-LDH particles are made of regular and hexagonal sheets [39]. Moreover, the SEM images of the MgAl CO_3-LDH@Asn biocatalyst indicated that almost all nanoparticles are in the form of stacked hexagonal plates with a diameter of 43–73 nm. It can also be concluded that the MgAl CO_3-LDH plates once

Table 1
Optimization of reaction conditions for the synthesis of 2, 4, and 5-(1H)-imidazoles.

Entry	Catalyst	Catalyst dosage (mg)	Solvent	Temperature (°C)	Time (min)	Yield (%)
	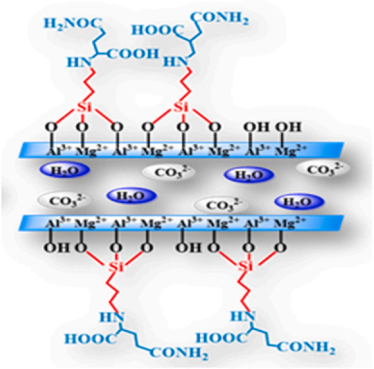					
1	MgAl CO_3-LDH@Asn	0.00	EtOH	Reflux	120	–
2	MgAl CO_3-LDH@Asn	20.00	–	Reflux	120	50
3	MgAl CO_3-LDH@Asn	20.00	MeCN	Reflux	20	65
4	MgAl CO_3-LDH@Asn	20.00	CH_2Cl_2	Reflux	20	–
5	MgAl CO_3-LDH@Asn	20.00	EtOH	Reflux	20	98
6	MgAl CO_3-LDH@Asn	20.00	H_2O	Reflux	20	60
7	MgAl CO_3-LDH@Asn	20.00	MeOH	Reflux	20	80
8	MgAl CO_3-LDH@Asn	10.00	EtOH	Reflux	20	70
9	MgAl CO_3-LDH@Asn	15.00	EtOH	Reflux	20	83
10	MgAl CO_3-LDH@Asn	30.00	EtOH	Reflux	20	90
11	MgAl CO_3-LDH@Asn	20.00	EtOH	r.t	20	–
14	MgAl CO_3-LDH	20.00	EtOH	Reflux	120	55
15	L-asparagine	20.00	EtOH	Reflux	20	75

Reaction conditions: benzyl (1 mmol), benzaldehyde (1 mmol), ammonium acetate (5 mmol), and biocatalyst in solvent (5 mL).

composed with L-asparagine have irregular dispersion (Fig. 3c–e). Based upon the corresponding histogram diagram (Fig. 3f), the average size of the MgAl CO_3-LDH@Asn nanoparticles was found to be in the range of 30–35 nm, which is almost in accordance with the particle size calculated by the Debye-Sherrer formula in XRD results (section 3.1.2).

3.1.4. EDX and elemental mapping analysis

To investigate the composition percentage of the MgAl CO_3-LDH@Asn, the energy dispersive X-ray analysis (EDX) was performed (Fig. 4). The EDX analysis illustrated the incorporation of C, O, N, Al, Mg, and Si elements into the structure of the as-prepared nanocomposite with elemental values of 11.78, 53.59, 3.29, 11.16, 18.94, and 1.24 %, respectively. The absence of chlorine in this analysis leads to the conclusion that the terminal chlorine in the chloropropyl trimethoxysilane bond chain has been completely substituted by the amine group of L-asparagine. Upon examination of all the mapping images (Fig. S1), the presence of C, O, N, Al, Mg, and Si elements in the structure of the as-prepared nanocomposite was detected. Furthermore, the dispersed and extremely insignificant coating of L-asparagine amino acid on the modified surface of MgAl CO_3-LDH was confirmed. It can be concluded that the elemental mapping of components in the MgAl CO_3-LDH@Asn conforms to the percentages reported by the EDX analysis.

3.1.5. TGA analysis

The thermal stability of MgAl CO_3-LDH@Asn biocatalyst was investigated *via* TGA analysis under oxygen atmosphere and temperature range of 25–800 °C, which is shown in Fig. 5. The first weight loss in the temperature range below 200 °C is due to the evaporation of absorbed water in the inner layers of the LDH, and also the removal of the remaining organic solvents in the structure of the MgAl CO_3-LDH@Asn biocatalyst [40]. The second weight loss that occurs in the temperature range of 200–500 °C is related to dehydroxylation and removal of carbonate ions from the inner layers and degradation of asparagine [41]. The third weight loss in the temperature range of 500–600 °C is associated with the destruction of the silane portion. Finally, at temperatures greater of 600 °C, the structure of the LHD is destroyed and metal oxides are formed. These results indicate that L-asparagine is successfully immobilized on the CPTMS-modified LDH.

3.2. Optimizing the reaction conditions

To assess the optimal value of reaction factors, a variety of parameters, including the amount of biocatalyst, type of solvent, reaction time and temperature were examined (Table 1). The reaction between benzyl (1 mmol), benzaldehyde (1 mmol), ammonium acetate (5 mmol), and biocatalyst in solvent (5 mL) for the synthesis of *tri*-substituted derivatives of 2, 4, 5-(H1)-imidazoles was considered to be a model reaction with or without biocatalysts under various conditions. The reaction progression was controlled by

Table 2
Synthesis of tri-substituted derivatives of 2, 4, 5-(H1)-imidazoles.

Entry	R group	Product	Reaction Time (min)	MP (°C)	MP (°C), ref.	Efficiency (%)
1	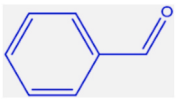	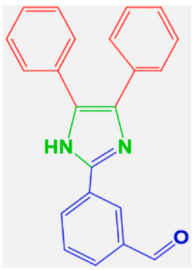	20	270–271	270-272 [42]	98
		4a				
2	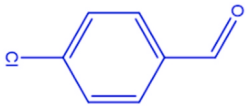	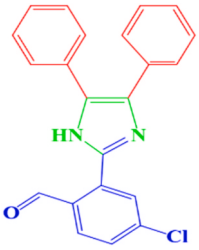	25	261–263	260-262 [42]	92
		4b				
3	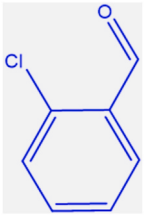	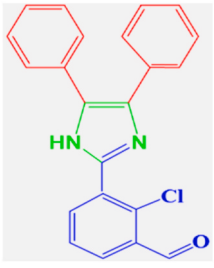	30	198–200	197-199 [42]	95
		4c				

(*continued on next page*)

Table 2 (*continued*)

Entry	R group	Product	Reaction Time (min)	MP (°C)	MP (°C), ref.	Efficiency (%)
4	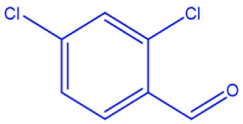	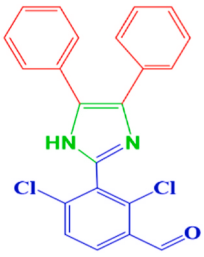	30	176–178	177-178 [43]	97
5	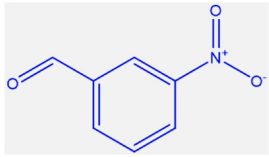	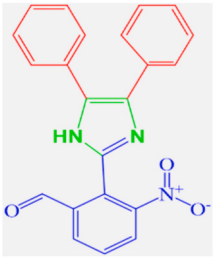	35	297–300	301-302 [43]	85
6	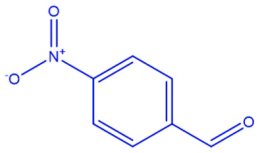	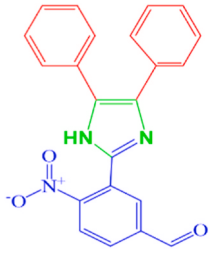	35	200–201	200-202 [42]	80

4d

4e

4f

(*continued on next page*)

Table 2 (*continued*)

Entry	R group	Product	Reaction Time (min)	MP (°C)	MP (°C), ref.	Efficiency (%)
7	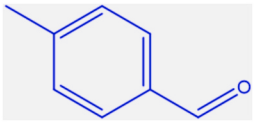	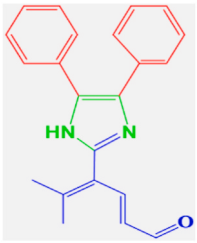	20	233–235	232-235 [44]	96
8	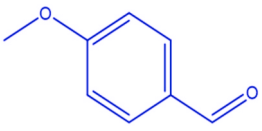	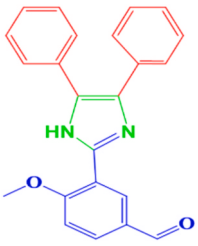	30	255–258	256-257 [41]	87
9	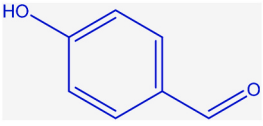	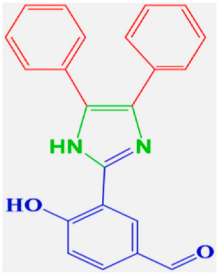	35	227–229	227-228 [41]	90

4g

4h

4i

(*continued on next page*)

Table 2 (*continued*)

Entry	R group	Product	Reaction Time (min)	MP (°C)	MP (°C), ref.	Efficiency (%)
10	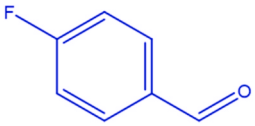	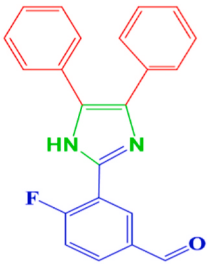	30	250–252	250-251 [42]	87
11	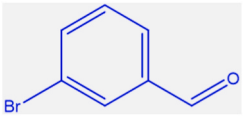	4j 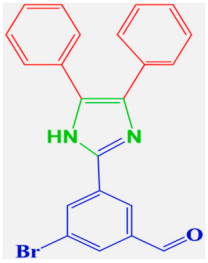	35	299–301	301-302 [44]	90
12	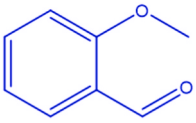	4k 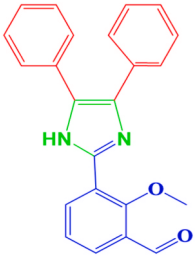	25	202–203	200-202 [41]	92
		4l				

Reaction conditions: benzyl (1 mmol), benzaldehyde (4a-l) (1 mmol), ammonium acetate (5 mmol), and biocatalyst in EtOH (20 mg) under reflux conditions.

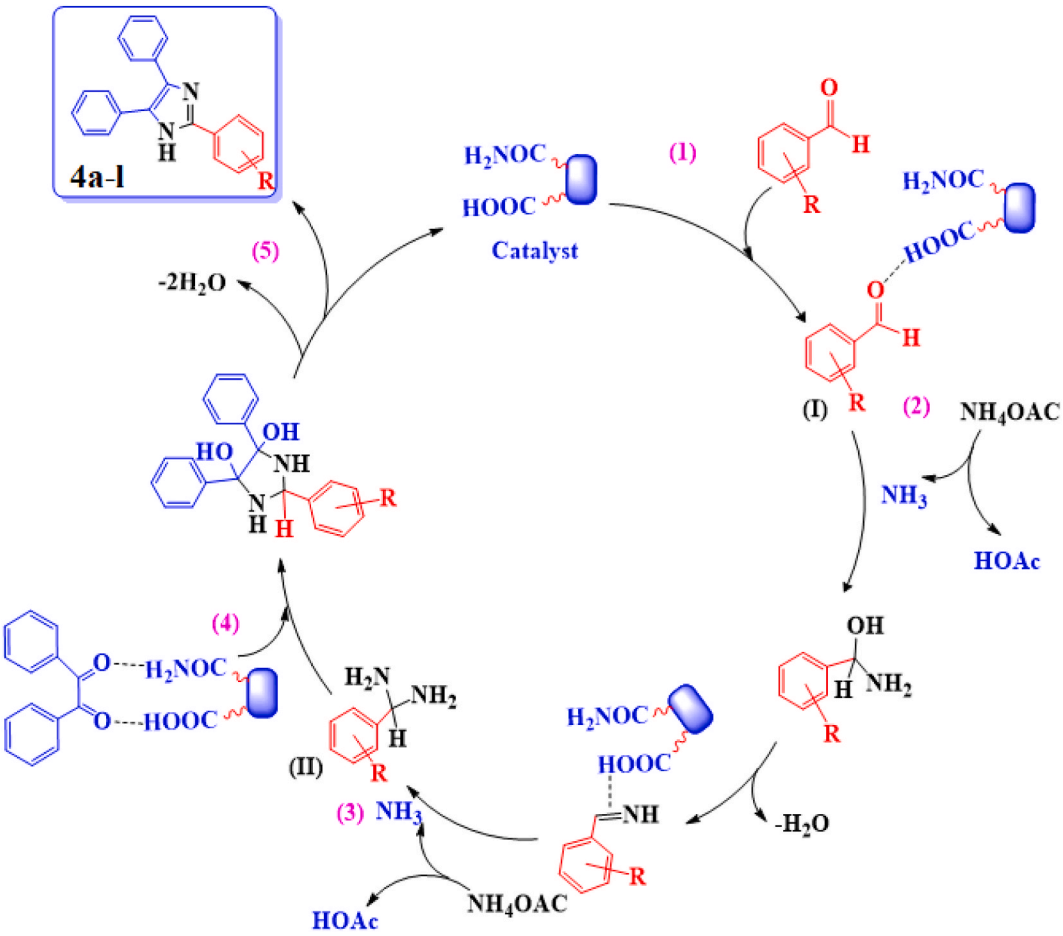

Scheme 3. The suggested reaction mechanism for the synthesizing of *tri*-substituted derivatives of 2, 4, 5-(H1)-imidazoles in the presence of MgAl CO_3-LDH@Asn biocatalyst.

TLC chromatography. Initially, the reaction was conducted in an ethanol solvent, reflux temperature, with 40 mg of MgAl CO_3-LDH@Asn biocatalyst. In this condition, the outputs were obtained with efficiencies of 85 %. To improve the reaction efficiency, the use of various solvents and solvent-free conditions was investigated. The results showed that the highest efficiency was achieved in the ethanol solvent (Entry 5). In the following step, the effect of the amount of the MgAl CO_3-LDH@Asn biocatalyst in the synthesis reaction of the *tri*-substituted derivatives of imidazoles was performed in the presence of 10,15, 20, 30 mg of biocatalyst. According to the experimental findings reported in Table 1, the optimum MgAl CO_3-LDH@Asn biocatalyst amount for the experiment was considered 20 mg. The blank experiment (biocatalyst dosage = 0.00 g) demonstrated that the reaction did not progress in the absence of the catalyst within the reported time (Entry 1). Studies were also carried out with a view to optimize the reaction time and temperature. The highest reaction yield was achieved within 20 min at reflux temperature. Finally, after optimizing the model reaction conditions, the reaction for the synthesis of *tri*-substituted derivatives of 2, 4, 5-(H1)-imidazoles using MgAl CO_3-LDH@Asn as a biocatalyst was investigated.

3.3. Development of optimal conditions for synthesizing other tri-substituted derivatives of imidazoles

After optimization of model reaction conditions for the synthesizing of *tri*-substituted derivatives of imidazole, this reaction was investigated using different aromatic aldehydes with electron donation and withdrawal groups. The findings obtained are presented in Table 2. According to the obtained results, it can be concluded that aromatic aldehydes with different substitutions have a significant effect on product yield, which can be justified considering the nature of the substituted groups and the steric hindrance effect.

3.4. Suggested pathway of the reaction mechanism

As illustrated in Scheme 3, the proposed mechanism for the synthesizing of imidazole derivatives is shown. As a starting point, ammonium acetate is segmented into acetic acid and ammonia. Next, acid protons from the L-asparagine COOH functional groups

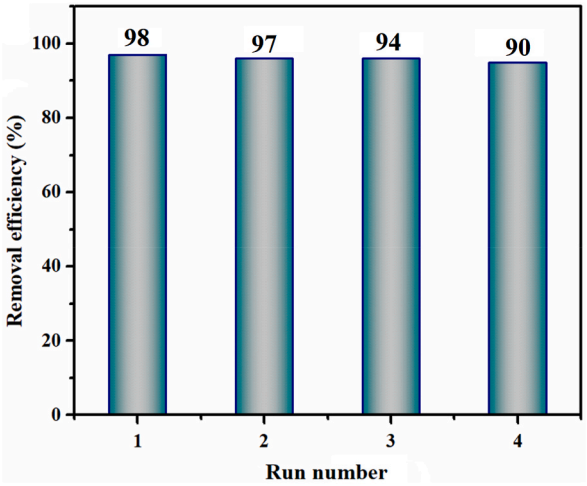

Fig. 6. Reusability efficiency of MgAl CO_3-LDH@Asn biocatalyst for the synthesis of *tri*-substituted derivatives of 2, 4, 5-(H1)-imidazoles after first, second, third, and fourth recyclability.

Table 3
Comparison of catalytic activity of various catalysts under different conditions for the synthesis of *tri*-substituted derivatives of 2, 4, 5-(H1)-imidazoles.

Entry	Catalyst	Solvent/Temperature	Time (min)	Yield (%)	Ref.
1	Cellulose/Fe_2O_3/Ag (0.015 g)	Solvent-Free/100 °C	10	91	[45]
2	L-Proline (15 % mol)	MeOH/Reflux	540	90	[46]
3	Silica sulfuric acid (0.5 g)	H_2O/Reflux	240	73	[47]
4	$TiCl_4.SiO_2$ (50 mol%)	Solvent-Free/110 °C	300	92	[48]
5	Fe_3O_4@PVA-SO_3H (0.5 g)	EtOH/r.t	40	98	[41]
6	ZrO_2-β-CD (40 % mol)	Solvent-Free/100 °C	24	96	[49]
7	ZnS–$ZnFe_2O_4$ (0.02 g)	Ultrasonic/70 °C	15	95	[44]
8	MgAl CO_3-LDH@Asn	EtOH/Reflux	20	98	This work

activate the carbonyl aldehyde and benzyl groups like Brønsted acids supported on the surface of the nanocomposite. With the nucleophilic attack of ammonia formed through the dissociation of ammonium acetate to the activated carbonyl group of aryl aldehyde, aryl aldimine is formed. Subsequently, the MgAl CO_3-LDH@Asn biocatalyst produces intermediate (II) by increasing the electrophilicity of the C=N bond on the aryl aldimine through the nucleophilic attack of ammonia. Afterward, the MgAl CO_3-LDH@Asn biocatalyst enables the carbonyl groups of benzyls to carry out the cycloaddition reaction with an intermediary (II). Finally, upon removal of the water molecule, the desired compound is formed.

3.5. *Recovery of the MgAl CO_3-LDH@Asn biocatalyst*

One of the advantages of heterogeneous catalysts is the possibility of easily separating and reusing them from the reaction mixture. In this regard, the recyclability of the biocatalyst (MgAl CO_3-LDH@Asn) was investigated in the model reaction (Fig. 6). After completing the reaction, the biocatalyst was centrifuged and washed with MeOH. Afterward, it was dried at temperature of 60 °C, and went into the following reaction without further purification. The biocatalyst (MgAl CO_3-LDH@Asn) could be reused four times without significantly diminishing its catalytic performance. The data presented in Fig. 6 demonstrated a gradual decline in reaction yield from 98 % to 90 % over four successive runs.

In order to evaluate the ability and efficiency of this method and catalyst, a comparison was conducted with previous methods for the synthesizing of *tri*-substituted derivatives of 2, 4, 5-(H1)-imidazoles (Table 3). Among the various biocatalysts, the best efficiency was related to MgAl CO_3-LDH@Asn biocatalyst according to the reaction conditions. Furthermore, the MgAl CO_3-LDH@Asn biocatalyst offers the benefits of short time, and high performance compared to other catalysts.

4. Conclusions

In summary, a new nanocomposite, MgAl CO_3-LDH@Asn, was successfully prepared by three-component reaction of MgAl CO_3-layered double hydroxide (LDH), 3-(chloropropyl) trimethoxysilane (CPTMS), and L-asparagine amino acid (Asn) *via* urea-assisted co-precipitation method. Various analyses, including FT-IR, XRD, SEM, EDX, and TGA were carried out to assess its proper synthesis and immobility. The MgAl CO_3-LDH@Asn nanocomposite was introduced as an efficient heterogeneous catalyst for the synthesizing of *tri*-

substituted derivatives of 2, 4, 5-(H1)-imidazoles. It was observed that high-efficiency products were obtained through 20 mg of MgAl CO_3-LDH@Asn biocatalyst in EtOH solvent within a short period of time (20 min). The high catalytic activity of the MgAl CO_3-LDH@Asn was maintained with only a slight loss over five cycles. The benefits of this research include the use of a biodegradable nanocatalyst without toxic transition metals, and the simplicity and low cost of the test method.

Data availability

Data will be made available on request.

CRediT authorship contribution statement

Shahram Moradi: Methodology, Investigation, Data curation. **Hadi Hassani Ardeshiri:** Writing – original draft, Software, Investigation, Formal analysis. **Alireza Gholami:** Software, Investigation. **Hossein Ghafuri:** Writing – review & editing, Visualization, Validation, Supervision, Project administration, Conceptualization.

Declaration of competing interest

The authors declare that they have no known competing financial interests or personal relationships that could have appeared to influence the work reported in this paper.

Appendix A. Supplementary data

Supplementary data to this article can be found online at https://doi.org/10.1016/j.heliyon.2023.e22185.

References

[1] Y. Cao, S. Jin, D. Zheng, C. Lin, Facile fabrication of ZnAl layered double hydroxide film co-intercalated with vanadates and laurates by one-step post modification, Coll. Interf. Sci. Commun. 40 (2021), 100351.
[2] L.N. Stepanova, E.O. Kobzar, N.N. Leont'eva, T.I. Gulyaeva, A.V. Vasilevich, A.V. Babenko, O.B. Belskaya, Study of the chemical and phase transformations in the mechanochemical synthesis of the MgAl-layered double hydroxide, J. Alloys Compd. 890 (2022), 161902.
[3] R. Benhiti, A. Ait Ichou, A. Zaghloul, R. Aziam, G. Carja, M. Zerbet, M. Chiban, Synthesis, characterization, and comparative study of MgAl-LDHs prepared by standard coprecipitation and urea hydrolysis methods for phosphate removal, Environ. Sci. Pollut. Res. 27 (2020) 45767–45774.
[4] A. Zaghloul, R. Benhiti, M.H. Abali, A. Ait Ichou, A. Soudani, M. Chiban, F. Sinan, Kinetic, isotherm, and thermodynamic studies of the removal of methyl orange by synthetic clays prepared using urea or coprecipitation, Euro-Mediterr. j. environ. integr. 6 (2021) 1–10.
[5] S. Nouaa, R. Aziam, R. Benhiti, G. Carja, S. Iaich, M. Zerbet, M. Chiban, Synthesis of LDH/Alginate composite beads as a potential adsorbent for phosphate removal: kinetic and equilibrium studies, Chem. Pap. (2023) 1–17.
[6] A.V. Karim, A. Hassani, P. Eghbali, P.V. Nidheesh, Nanostructured modified layered double hydroxides (LDHs)-based catalysts: a review on synthesis, characterization, and applications in water remediation by advanced oxidation processes, Curr. Opin. Solid State Mater. Sci. 26 (1) (2022), 100965.
[7] M.V. Bukhtiyarova, A review on effect of synthesis conditions on the formation of layered double hydroxides, J. Solid State Chem. 269 (2019) 494–506.
[8] C. Forano, T. Hibino, F. Leroux, C. Taviot-Guého, Layered double hydroxides, Dev. Clay Sci. 1 (2006) 1021–1095.
[9] J. Mittal, Recent progress in the synthesis of Layered Double Hydroxides and their application for the adsorptive removal of dyes: a review, J. Environ. Manage. 295 (2021), 113017.
[10] H.N. Tran, D.T. Nguyen, G.T. Le, F. Tomul, E.C. Lima, S.H. Woo, H.P. Chao, Adsorption mechanism of hexavalent chromium onto layered double hydroxides-based adsorbents: a systematic in-depth review, J. Hazard Mater. 373 (2019) 258–270.
[11] G. Mishra, B. Dash, S. Pandey, Layered double hydroxides: a brief review from fundamentals to application as evolving biomaterials, Appl. Clay Sci. 153 (2018) 172–186.
[12] K. Yan, G. Wu, W. Jin, Recent advances in the synthesis of layered, double-hydroxide-Based materials and their applications in hydrogen and oxygen evolution, Energy Technol. 4 (3) (2016) 354–368.
[13] M. Suárez-Quezada, G. Romero-Ortiz, J.E. Samaniego-Benítez, V. Suárez, A. Mantilla, H_2 production by the water splitting reaction using photocatalysts derived from calcined ZnAl LDH, Fuel 240 (2019) 262–269.
[14] Y. Wu, Y. Gong, J. Liu, T. Chen, Q. Liu, Y. Zhu, S. Xu, Constructing NiFe-LDH wrapped Cu_2O nanocube heterostructure photocatalysts for enhanced photocatalytic dye degradation and CO_2 reduction via Z-scheme mechanism, J. Alloys Compd. 831 (2020), 154723.
[15] X. Feng, Y. Shi, J. Shi, L. Hao, Z. Hu, Superhydrophilic 3D peony flower-like Mo-doped Ni_2S_3@NiFe LDH heterostructure electrocatalyst for accelerating water splitting, Int. J. Hydrog. Energy. 46 (7) (2021) 5169–5180.
[16] Z.Z. Yang, C. Zhang, G.M. Zeng, X.F. Tan, H. Wang, D.L. Huang, K. Nie, Design and engineering of layered double hydroxide-based catalysts for water depollution by advanced oxidation processes: a review, J. Mater. Chem. A. 8 (8) (2020) 4141–4173.
[17] Z. Tang, Z. Qiu, S. Lu, X. Shi, Functionalized layered double hydroxide applied to heavy metal ions absorption: a review, Nanotechnol. Rev. 9 (1) (2020) 800–819.
[18] B. Keita, A. Belhouari, L. Nadjo, Oxometalate-clay-modified electrodes: synthesis and properties of anionic clays pillared by metatungstate, J. Electroanal. Chem. 355 (1–2) (1993) 235–251.
[19] E. Goldberg, Amino acid composition and properties of crystalline lactate dehydrogenase X from mouse testes, J. Biol. Chem. 247 (7) (1972) 2044–2048.
[20] D.M. Gwinn, A.G. Lee, M. Briones-Martin-del-Campo, C.S. Conn, D.R. Simpson, A.I. Scott, E.A. Sweet-Cordero, Oncogenic KRAS regulates amino acid homeostasis and asparagine biosynthesis via ATF_4 and alters sensitivity to L-asparaginase, Cancer Cell 33 (1) (2018) 91–107.
[21] D.A. Cooney, R.E. Handschumacher, L-asparaginase and L-asparagine metabolism, Annu. Rev. Pharmacol. 10 (1) (1970) 421–440.
[22] N. Thimmaraju, S.M. Shamshuddin, Synthesis of 2, 4, 5-trisubstituted imidazoles, quinoxalines and 1, 5-benzodiazepines over an eco-friendly and highly efficient ZrO_2–Al_2O_3 catalyst, RSC Adv. 6 (65) (2016) 60231–60243.
[23] S.S. Dipake, V.D. Ingale, S.A. Korde, M.K. Lande, A.S. Rajbhoj, S.T. Gaikwad, An efficient green protocol for the synthesis of 1, 2, 4, 5-tetrasubstituted imidazoles in the presence of ZSM-11 zeolite as a reusable catalyst, RSC Adv. 12 (7) (2022) 4358–4369.

[24] S.Y. Cao, Y. Zhou, Y.X. Ma, S.X. Cheng, G.M. Tang, Y.T. Wang, Syntheses, crystal structure, luminescent behaviors and Hirshfeld surface of salts with imidazole and benzimidazole-yl scaffolds, J. Mol. Struct. 1276 (2023), 134764.
[25] H.V. Tolomeu, C.A.M. Fraga, Imidazole: synthesis, Functionalization and physicochemical properties of a privileged structure in medicinal Chemistry, Molecules 28 (2) (2023) 838.
[26] M. Ara, H. Ghafuri, N. Ghanbari, Copper (II) anchored on layered double hydroxide functionalized guanidine as a heterogeneous catalyst for the synthesis of tetrazole derivatives, Coll. Interf. Sci. Commun. 53 (2023), 100704.
[27] Q. Wang, Y. Feng, J. Feng, D. Li, Enhanced thermal-and photo-stability of acid yellow 17 by incorporation into layered double hydroxides, J. Solid State Chem. 184 (6) (2011) 1551–1555.
[28] K. Tamura, R. Kawashiri, N. Iyi, Y. Watanabe, H. Sakuma, M. Kamon, Rosette-like layered double hydroxides: adsorbent materials for the removal of anionic pollutants from water, ACS Appl. Mater. Interfaces 11 (31) (2019) 27954–27963.
[29] N. Ghanbari, H. Ghafuri, Design and preparation of nanoarchitectonics of LDH/polymer composite with particular morphology as catalyst for green synthesis of imidazole derivatives, Sci. Rep. 12 (1) (2022) 1–15.
[30] G. Zheng, C. Wu, J. Wang, S. Mo, Z. Zou, B. Zhou, F. Long, Space-confined effect one-pot synthesis of γ-AlO(OH)/MgAl-LDH heterostructures with excellent adsorption performance, Nanoscale Res. Lett. 14 (2019) 1–12.
[31] Y. Feng, D. Li, Y. Wang, D.G. Evans, X. Duan, Synthesis and characterization of a UV absorbent-intercalated Zn–Al layered double hydroxide, Polym, Degrad. Stab. 91 (4) (2006) 789–794.
[32] E.J. Baran, I. Viera, M.H. Torre, Vibrational spectra of the Cu (II) complexes of L-asparagine and L-glutamine, Spectrochim. Acta: Mol. Biomol. Spectrosc. 66 (1) (2007) 114–117.
[33] S. Chen, Y. Xu, Y. Tang, W. Chen, S. Chen, L. Hu, G. Boulon, Pretreatment by recyclable Fe3O4@Mg/Al-CO_3-LDH magnetic nano-adsorbent to dephosphorize for the determination of trace F^- and Cl^- in phosphorus-rich solutions, RSC Adv. 10 (72) (2020) 44361–44372.
[34] S. Kumari, N. Thakur, R. Kumar, R.C. Thakur, A. Sharma, Effect of synthetic parameters on crystallinity of hydrotalcite-like anionic clays with elucidation and identification through X-ray diffraction analysis, ECS Trans. 107 (1) (2022), 18903.
[35] M.A. Rezvani, S. Hosseini, H. Hassani Ardeshiri, Highly efficient catalytic oxidative desulfurization of gasoline using $PMnW_{11}$@PANI@CS as a new inorganic–organic hybrid biocatalyst, Energy Fuels 36 (14) (2022) 7722–7732.
[36] M.A. Rezvani, M. Aghmasheh, A. Hassani, H. Hassani Ardeshiri, Synthesis and characterization of a new hybrid nanocomposite based on di-substituted heteropolyanion-quantum dots as a high-performance biocatalyst for organic dye removal from wastewater, J. Coord. Chem. 75 (3–4) (2022) 507–523.
[37] M. Shaterian, M. Yulchikhani, Z. Aghasadeghi, H.H. Ardeshiri, Synthesis, characterization, and investigation of electrochemical hydrogen storage capacity in barium hexaferrite nanocomposite, J. Alloys Compd. 915 (2022), 165350.
[38] E. Alibakhshi, E. Ghasemi, M. Mahdavian, B. Ramezanzadeh, Corrosion inhibitor release from Zn-Al-[PO_4^{3-}]-[CO_3^{2-}] layered double hydroxide nanoparticles, Prog. Color. Color. Coat 9 (4) (2016) 233–248.
[39] C. Simari, E. Lufrano, A. Brunetti, G. Barbieri, I. Nicotera, Highly-performing and low-cost nanostructured membranes based on Polysulfone and layered doubled hydroxide for high-temperature proton exchange membrane fuel cells, J. Power Sources 471 (2020), 228440.
[40] G. Carja, G. Delahay, Mesoporous mixed oxides derived from pillared oxovanadates layered double hydroxides as new catalysts for the selective catalytic reduction of NO by NH_3, Appl. Catal. B Environ. 47 (1) (2004) 59–66.
[41] A. Maleki, J. Rahimi, K. Valadi, Sulfonated Fe_3O_4@PVA superparamagnetic nanostructure: design, in-situ preparation, characterization and application in the synthesis of imidazoles as a highly efficient organic–inorganic Bronsted acid catalyst, Nano-Struct. Nano-Objects. 18 (2019), 100264.
[42] M. Kalhor, Z. Zarnegar, Fe_3O_4/SO_3H@Zeolite-Y as a novel multi-functional and magnetic biocatalyst for clean and soft synthesis of imidazole and perimidine derivatives, RSC Adv. 9 (34) (2019) 19333–19346. .
[43] S.A. Dake, M.B. Khedkar, G.S. Irmale, S.J. Ukalgaonkar, V.V. Thorat, S.A. Shintre, R.P. Pawar, Sulfated tin oxide: a reusable and highly efficient heterogeneous catalyst for the synthesis of 2, 4, 5-triaryl-1 H-imidazole derivatives, Synth. Commun. 42 (10) (2012) 1509–1520. .
[44] Z. Varzi, A. Maleki, Design and preparation of ZnS-$ZnFe_2O_4$: a green and efficient hybrid biocatalyst for the multicomponent synthesis of 2, 4, 5-triaryl-1H-imidazoles, Appl. Organomet. Chem. 33 (8) (2019), e5008.
[45] A. Maleki, H. Movahed, R. Paydar, Design and development of a novel cellulose/γ-Fe_2O_3/Ag nanocomposite: a potential green catalyst and antibacterial agent, RSC Adv. 6 (17) (2016) 13657–13665.
[46] S. Samai, G.C. Nandi, P. Singh, M.S. Singh, L-Proline, An efficient catalyst for the one-pot synthesis of 2, 4, 5-trisubstituted and 1, 2, 4, 5-tetrasubstituted imidazoles, Tetrahedron 65 (49) (2009) 10155–10161.
[47] A. Shaabani, A. Rahmati, Silica sulfuric acid as an efficient and recoverable catalyst for the synthesis of trisubstituted imidazoles, J. Mol. Catal. A: Chem. 249 (1–2) (2006) 246–248. .
[48] B.F. Mirjalili, A.H. Bamoniri, L. Zamani, One-pot synthesis of 1,2,4,5-tetrasubstituted imidazoles promoted by nano-$TiCl_4$. SiO_2, Sci. Iran. 19 (3) (2012) 565–568. .
[49] Y.R. Girish, K.S.S. Kumar, K.N. Thimmaiah, K.S. Rangappa, S. Shashikanth, ZrO_2-β-cyclodextrin catalyzed synthesis of 2, 4, 5-trisubstituted imidazoles and 1, 2-disubstituted benzimidazoles under solvent free conditions and evaluation of their antibacterial study, RSC Adv. 5 (92) (2015) 75533–75546.